Metascience in Aerospace

Metascience in Aerospace, 3(3): 97–110.
DOI: 10.3934/mina.2026007
Received date: 31 May 2026
Revised date: 15 September 2026
Accepted date: 09 October 2026
Published date: 02 November 2026

https://www.aimspress.com/journal/mina

Research article

Molniya-type orbits with possible application in Argentina

Jorge Lassig*

Departamento Mecánica Aplicada, Universidad Nacional del Comahue, Bs.As. 1400, (8300) Neuquén, Argentina

* **Correspondence:** Email: Jorge.lassig@fain.uncoma.edu.ar; Tel: +54-299-430-5359.

Abstract: The Molniya orbit is a highly elliptical orbit with an orbital period of several hours. A satellite in this orbit projects a large portion of its orbital time onto a specific area of the Earth, a phenomenon known as the "apogee dwell". These types of orbits are named after the Russian-Soviet Molniya series of communications satellites, which were launched starting in the mid-1960s. Possible applications of this type of orbit include communications and Antarctic weather monitoring. The original project was implemented during the development of Pehuensat-2, which was put on standby due to a lack of funding. Finally, as a preliminary implementation, it is proposed to use a 3U cubesat in a polar low earth orbit (LEO) orbit, which we will call Pehuensat-4, to test the deployment of the boom in flight, its degree of stability, the camera for taking images, its processing, and sending to the receiving station.

Keywords: Cubesat; Pehuensat; Molniya; Boom; Satellite image

1. Introduction

The Molniya orbit is a highly elliptical orbit with an inclination of 63.4° and an orbital period of approximately 12 hours [1]. A satellite in this orbit spends the majority of its time over a specific area of Earth, a phenomenon known as the "apogee dwell." These orbits take their name from the Russian Molniya series of communications satellites, which became operational in the 1960s [2].

For stationary apogees, the orbital period must divide the 24 hours into equal parts. An orbital period of 12 hours gives two apogees (i.e., when the satellite reaches apogee it is always over one of the two fixed points on Earth) and two perigees; an orbital period of 6 hours will result in four perigees and four apogees.

The large orbital inclination allows the apogee to be located near either the North or South Pole, where coverage from a geostationary satellite is either poor or nonexistent. In general, the Earth's curvature perturbs the argument of perigee [3], so that even if it is located near a pole, it will be moving slowly unless the satellite's orbit is corrected with the corresponding burns. To avoid this fuel consumption, the Molniya orbit uses an inclination of 63.4°, an angle at which the perturbation is zero.

Figure 1 shows a Molniya orbit of 12 hours. If zero hour is located at perigee at about 1500 km altitude, then at 2 hours, it will be at an altitude of 23,000 km and at 6 hours, it will be at apogee at about 40,000 km altitude above the Earth's surface.

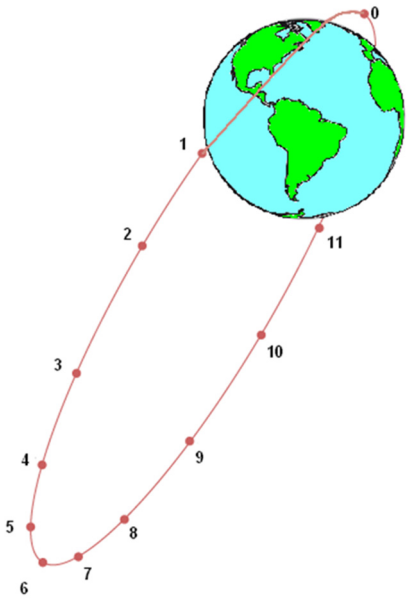


Figure 1. Molniya orbit for the Southern Hemisphere, where the numbers indicate the relative time.

2. Molniya Orbit

A simulation of a Molniya orbit over the Drake Passage was conducted, with the following orbital parameters:

Perigee altitude = 1500 km
Apogee altitude = 40,000 km
Eccentricity = 0.7096
Period = 12 hrs
Inclination = 63.4º
Ascending node longitude = 140º, and
Argument of perigee = 80º

The result was an orbit projected onto the Earth's surface as shown in Figure 2, featuring two apogees: one located over the Drake Passage and the other southwest of Australia, almost over Antarctica.

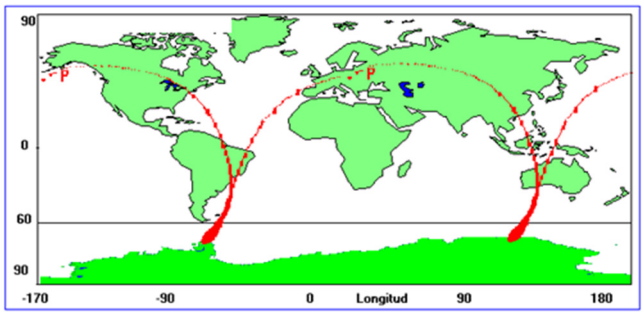


Figure 2. Molniya orbit of 12 hours, in one day it has two apogees and two perigees.

Table 1 shows the time and altitude above the Earth's surface according to the orbital position (true anomaly in degrees), and Figure 3 illustrates the satellite's location for a true anomaly of 150°.

Table 1. Molniya orbit.

Posición (º)	Tiempo (Hs)	Altitud (Km)
0	0	1500
30	0,1283	1964
60	0,29	3563
90	0,554	7090
120	1,118	14496
150	2,635	28561
180	6,176	40000
210	9,717	28562
240	11,234	14496
270	11,798	7090
300	12,062	3563
330	12,224	1964
360	12,352	1500

To meet Argentina's demand, two satellites would effectively cover 21 out of 24 hours for the two potential applications: communications and meteorology. From a meteorological standpoint, this is adequate; however, to maintain 24-hour coverage for communications, three satellites in an orbit yet to be determined would be required.

The mission would focus on Antarctic and high-latitude meteorology. A weather satellite located there could sequentially capture images of Antarctica. This information is vital for forecasting the movement of migratory lows, which are ultimately responsible for significant weather phenomena in the Southern Hemisphere, such as cold fronts, late frosts, and extreme winds, as well as for forecasting wind, rainfall, and droughts in this part of the world.

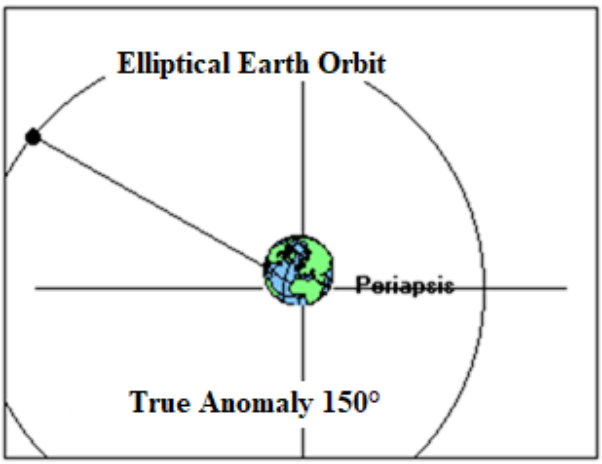


Figure 3. Orbital position given by the true anomaly.

From 120 degrees to 240 degrees, a visible coverage of 10.5 hours is achieved for the satellite. Figure 4 illustrates how the size of Antarctica varies from 23,000 km to its maximum extent (apogee).

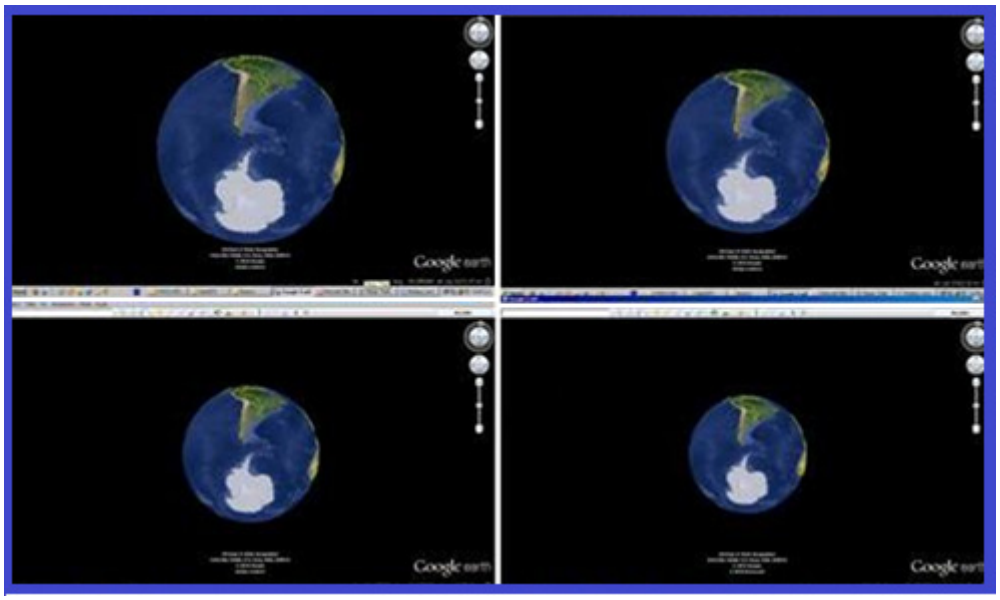


Figure 4. Satellite coverage from a Molniya orbit centered its apogee over the Antarctic Peninsula, from top to bottom, the heights correspond to 23,000, 28,500, 34,000 and 40,000 Km.

One of the characteristics of the Southern Hemisphere compared to the Northern Hemisphere is its low percentage of landmass. This results in fewer fixed weather stations, leading to a significant lack of data for weather forecasting models. It is a well-known fact that forecast errors in the Southern Hemisphere are greater than in the Northern Hemisphere for this reason.

In particular, a series of weather satellites that are equipped with radio transmitters would be of great help for communications throughout Antarctica.

3. How to do it?

A satellite using a Molniya orbit, as described in Section 2 of this paper, will have to cross the Van Allen radiation belts; therefore, radiation shielding must be carefully considered. Furthermore, this type of orbit requires relatively complex receiving stations, such as those with azimuth and elevation tracking capabilities, and high gain at the orbit's apogee.

Therefore, the project should be carried out in two phases: the first phase will demonstrate the technology to be used in a polar low earth orbit (LEO) orbit using a 3U cubesat; and the second phase, once the system engineering is validated, a smaller, more radiation-resistant satellite, which has already been flight-tested, will be used.

3.1. Phase A

For this, a 3U cubesat in a polar LEO orbit (Figure 5), which we will call Pehuensat-4, will be used to test the boom deployment and its stability in flight; additionally, the camera for image capture, processing, and transmission to the receiving station will be tested.

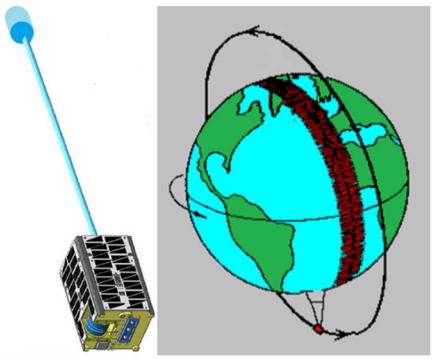


Figure 5. Phase A: Pehuensat-4, will be a 3U CubeSat in Polar orbit at 800 Km.

3.1.1. Image Acquisition

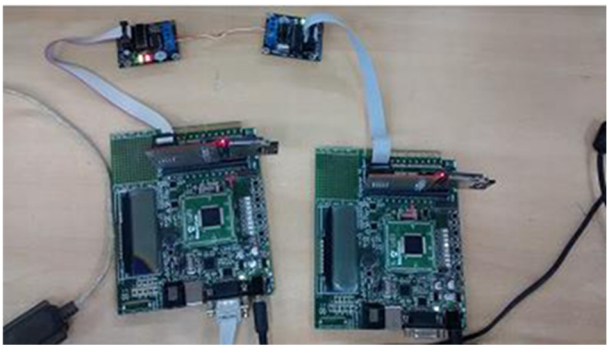


Figure 6. Explorer16 boards with CAN boards.

Ensuring a secure and reliable communication medium for space applications led to the decision

to evaluate the controller area network (CAN) protocol, specifically applied to image transmission [4]. To this end, Explorer 16 boards with their corresponding P24F128GA010 microcontrollers were used, along with CAN protocol boards featuring their respective transceivers (MCP2551) and controllers (MCP2515), as shown in Figure 6; two secure digital (SD) modules were also employed.

The (SD) standard is favorably adopted as one of the most common mass storage media for digital cameras and many other consumer multimedia applications.

3.1.2. Focus control in a video camera

The unit was designed with the following criteria:

(a) communicating with other processing devices using different communication protocols;

(b) sensing the angular position of the lens by reading the value of a trimpot whose rotation is proportional to that of the lens; and

(c) controlling a DC motor to modify the angular position of the lens [5].

Details of the camera's exploded view and its assembly can be seen in Figure 7.

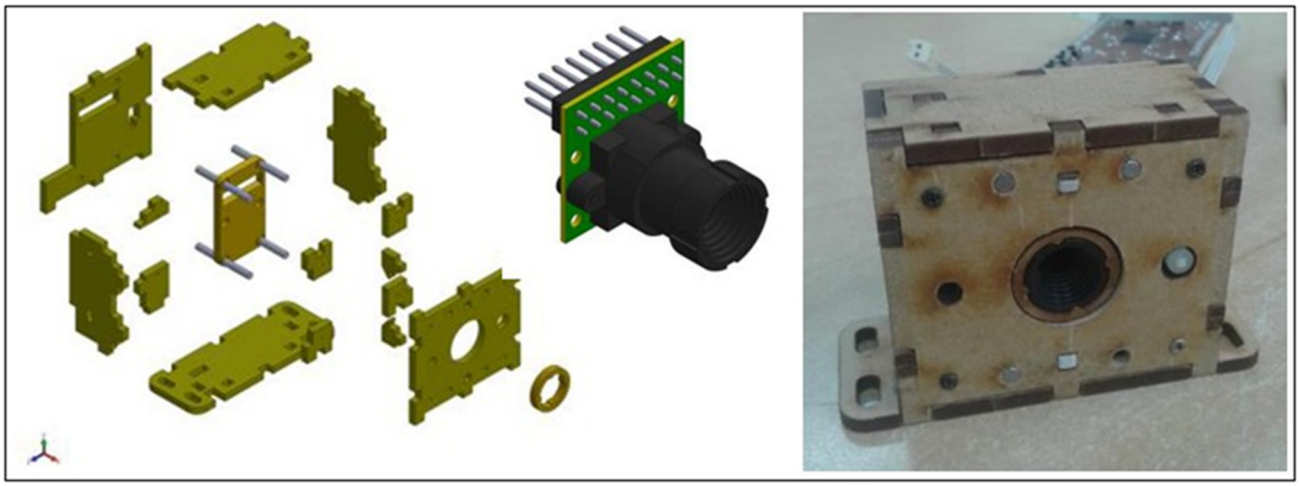


Figure 7. Tested prototype for focus control. Camera (center), with the detail of the mechanical support assembly (left), and the focus system with the camera mounted inside (right).

3.1.3. High-speed satellite data link communication.

The Pehuensat-4 will be a LEO satellite whose mission will consist of transmitting its telemetry to Earth and taking images from space for real-time (streaming) and delayed (storage and download) transmission [6]. Satellite control will be performed in the ultra high frequency (UHF) band (435 MHz). Data and image transmission will be in digital format in the S-band (2.4 GHz). Communications in this band will be downlink only. One of the protocols to be used for communication on the 2.4 GHz link is the one defined by the IEEE 802.11 standard for the physical and data link layers.

The images will be available in two different qualities: high and low. The worst condition of the communications system will be the download of high-quality images weighing up to 10 MBs.

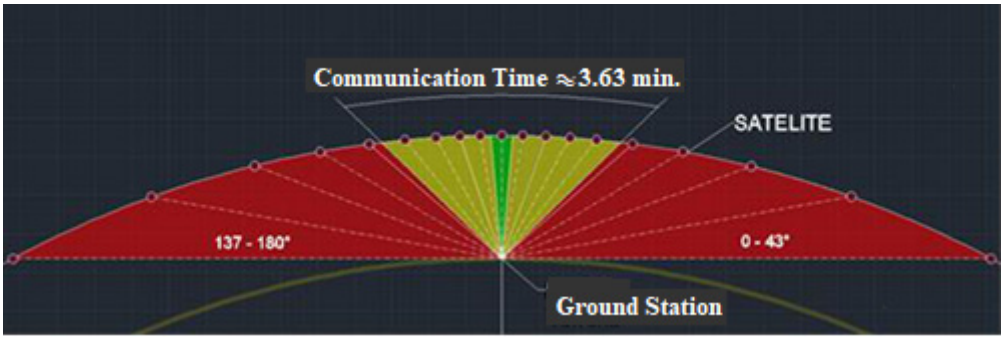


Figure 8. Satellite coverage over our image receiving station.

Given that the satellite will be visible for a short time within the ground antenna's range, as illustrated in Figure 8, the communication window will last a few seconds (estimated at 240 seconds). This timeframe is for downloading images; therefore, the necessary bandwidth must exceed 400 kbps. However, assuming command and processing times, a bandwidth that ensures a single-pass download should be on the order of 1024 kbps.

3.1.4. Patch Antenna at 2.4 GHz.

The transmitting antenna is a patch antenna with a gain of approximately 6 dB, as illustrated in Figure 9. The earth station antenna is a parabolic dish with an aperture efficiency of 0.55 and an estimated diameter of 0.9 m [7]. The bit rate for the downlink is set at 1 Mbps with quadrature phase shift keying (QPSK) modulation, the maximum allowable bit error rate (BER) is 10^{-6}, and the LEO orbit is estimated to be around 800 km. These parameters are shown in Table 2.

Table 2. Input parameters.

Input parameters	
Operating frequency (GHz)	2.4
Transmit power (Watts)	1
Transmitting antenna gain (dBi)	6.036
Diameter of the parabolic antenna of the ground station (m)	0.9
Aperture efficiency of the parabolic reflector	0.55
Estimated distance from LEO orbit (km)	800
Estimated system noise temperature (K)	139
Data bit rate (Mbps)	1
Digital modulation type	QPSK
Error rate per bit	10^{-6}

The triangular patch antenna with an FR4 substrate has a wide beamwidth. Beamwidth is crucial because the downlink antenna is fixed to the satellite and cannot be moved, always pointing towards the Earth's center. Therefore, a wide beamwidth is essential to ensure longer-lasting communication.

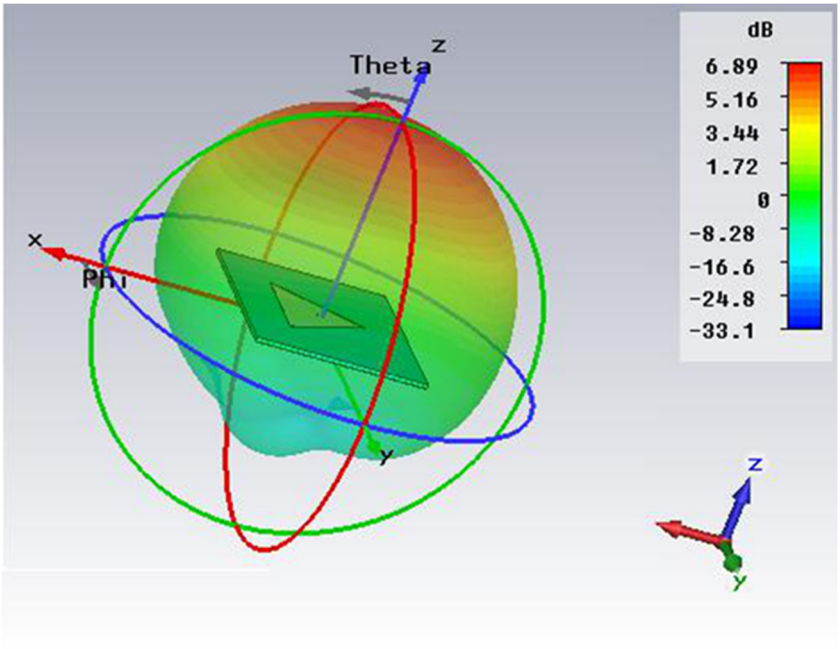


Figure 9. Antenna gain simulation.

3.1.5. Onboard computer

A Bleagle board with very high processing capacity and multiple peripheral ports will be used. Two boards (CB and PV) will be installed, one functioning as the onboard computer and the other as the video processing and image storage management board. In case of failure of the main board, the second board can take control of the satellite.

3.1.6. Information Storage

Data and image storage will be performed on solid state memory, SD cards. The goal is to store images in memory for subsequent transmission to the ground in successive passes, while also defining two operating modes: high-definition or standard definition. The high-definition mode (JPEG2000 protocol) will be a proprietary operating mode, selectable from the ground and with a scheduled operation. The standard definition version will be public and will allow the download of images in a single pass, with automatic triggering based on the satellite's operating status.

3.2. Phase B

A 14 kg nanosatellite is assembled using two Pehuensat-1 modules, as illustrated in Figure 10, and is designed to be placed in a Molniya orbit. The Pehuensat-1 module underwent flight testing and demonstrated excellent structural and thermal characteristics to house the electronic components. It was launched from India aboard the PSLV-C7 launch vehicle in 2007 [8].

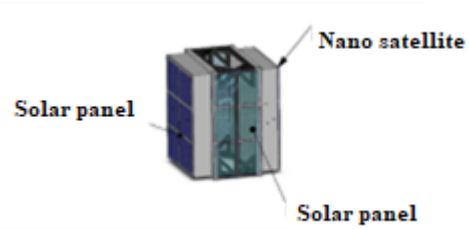


Figure 10. Preliminary structure of Pehuensat-2.

One module will carry the onboard computer and communications equipment; the other, module will carry the payload. The space between the modules would have room for passive attitude control, via a boom (top), and space for a camera (bottom). It is worth noting that Pehuensat-2 was developed between 2010 and 2015 following the flight and data analysis from the Pehuensat-1 mission in 2007.

3.2.1. Structure

Static analyses were performed (such as the one shown in Figure 11), followed by a dynamic study to determine the vibration frequencies and modes. A commercial finite element analysis software was used; the model employed a mesh consisting of 55,183 elements and 128,820 nodes [9].

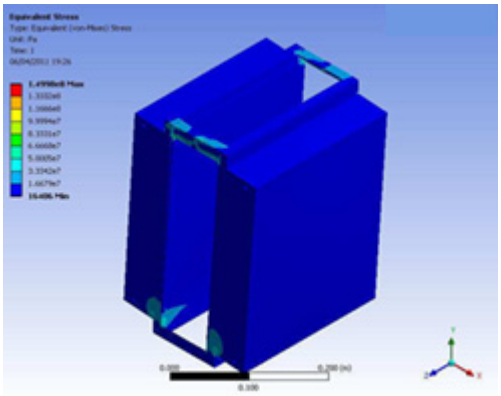


Figure 11. Equivalent voltage calculated using the Von Mises criterion. Unit: [Pa].

The complete structure measures 432 x 235 x 215 mm and is constructed from 6061 T6 aluminum. Each module contains a 3 mm thick plate that acts as a closure, secured to each module with screws. Tantalum coatings on the onboard computer housings will significantly reduce radiation to the electronic components.

3.2.2. Attitude control

In order to take images of the planet, it is necessary to have an attitude control, for this it was decided to use a passive system, consisting of a boom [10] that will extend once it is put into orbit.

Based on the satellite's mass, the boom would have a mass of two kilograms and a span of 2.16 m. The moments of inertia of the satellite with the boom extended will be as follows.

Ixx = 10.0358 (Kg m^2).
Iyy = 10.0400 (Kg m^2).
Izz = 0.0959 (Kg m^2).

To determine if this geometric configuration is stable, the coefficients Kx and Kz were determined as a function of the principal moments of inertia:

Kx = (Iyy – Izz) / Ixx. (1)
Kz = (Iyy – Ixx) / Izz. (2)
resulting in:
Kx = 0.9908.
Kz = 0.0427.

By referring to the stability diagram in Figure 12 [11], it can be deduced that the geometric configuration is stable; although the diagram shows it lying on the stability boundary, final adjustments to the boom's mass and/or length would shift the stabilization point further upward.

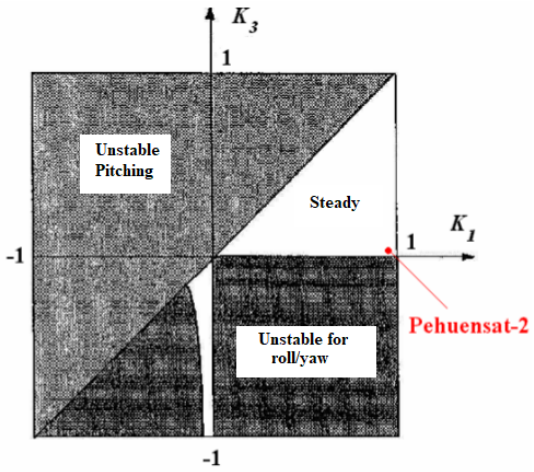


Figure 12. Diagram of stable regions by gravity gradient for low circular orbit satellites.

Typical perturbations that the satellite will encounter in a LEO orbit will be due to solar pressure, aerodynamic drag, magnetic torques due to variations in the Earth's magnetic field, and torques due to variations in the planet's gravity gradient.

All the aforementioned disturbances were calculated (Lassig, 2007), as well as the gravitational torque (Tgg) of the boom, and the following conclusions were reached. For a damping factor ζ=1 (extreme), stabilization is achieved in 23 minutes. For ζ=0.007 (ratio between Tcushioning/Tgg), stabilization occurs with an oscillation less than one in 6 days, and with an oscillation less than 0.01a in 15 days (see Figure 13).

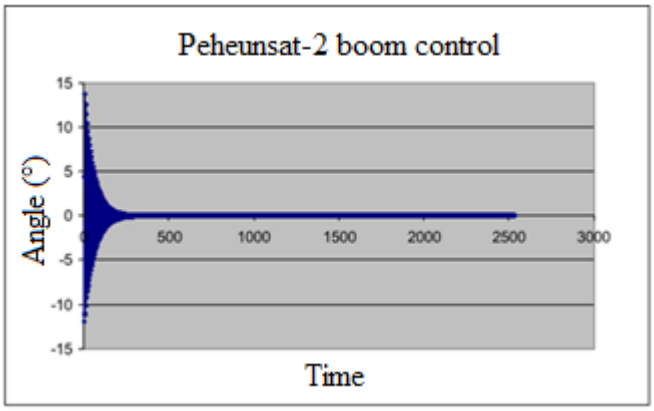


Figure 13. Boom response time, to vertically stabilize the satellite, after being deployed.

Finally, the satellite-boom arrangement is as shown in Figure 14.

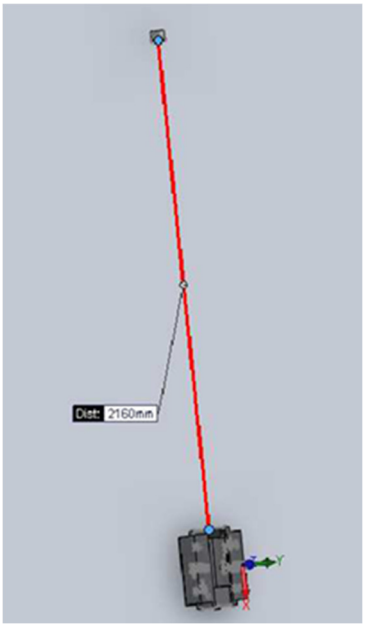


Figure 14. Pehuensat-2 with its extended boom.

3.2.3. Image Capture

The scientific mission of PehuenSat-2 will consist of carrying a camera to take images of the Earth's surface.

To do this, it is necessary to determine the following: (a) the spectral band, (b) the spatial resolution, and (c) the geographic coverage. Item (a) will determine the type of sensor, item (b) will determine he altitude of the satellite and the optics accompanying the sensor, and item (c) will determine the type of orbit.

Regarding the first objective, and based on the applications carried out at the Meteorological Satellite Imaging Laboratory at the National University of Comahue (LISaMet), the most frequently used band is the thermal infrared (IR) band (see Table 3); however, this type of sensor requires cooling,

which would complicate the mission, so it was decided to select a camera that operates in the visible and near-IR spectrum.

Table 3. Spectral bands used.

Spectral bands used			
Application	Visible	Near IR	Thermal IR
Frost			X
Lakes			X
Weather Forecast		X	X
Volcanoes	X		

For the second objective, it is advisable to improve the resolution by a factor of 100, meaning that the pixel should represent approximately 100 meters on each side, as indicated in Table 4.

Table 4. Current and ideal resolutions

Current and ideal resolutions		
Application	NOAA Resolution	Ideal Resolution (m)
Frost	1.100	100
Lakes	1.100	100 - 500
Weather Forecast	1.100	1.000
Volcanoes	1.100	100 -1.000

For objective (c), the orbit should cover the entire Argentine territory, which implies an inclination of at least 56º.

From the perspective of weather forecasting, it is advantageous to obtain imagery from the South Pacific, and ideally, data from Antarctica; since many systems affecting the region originate there, a polar orbit would be more suitable.

For all these reasons, the recommended orbit would be the Molniya orbit centered on the Drake Passage, as described in this paper, and a camera that scans the visible and near-infrared spectrum.

4. Discussion

The first phase, consisting of testing the technologies in flight using a 3U cubesat, can be carried out through our University, with the experience of having performed two space missions to date (PADE [12], and Peuensat-1 [13]).

For the second phase, given that Molniya satellites must pass through the radiation belt at least a couple of times a day, necessitating appropriate shielding, it is proposed to use a proprietary design consisting of two modules previously used on Pehuensat-1 and flight-tested, as they offer suitable temperature control and radiation protection capabilities. Furthermore, the electronic components must be of high quality and capable of surviving that space environment. Consequently, a satellite designed for the aforementioned meteorological or communications purposes would need to be built in collaboration with companies capable of handling such technologies.

Furthermore, since the contribution of meteorological data is free and used by the entire

international community, it would be very useful to partner with other countries in the Southern Hemisphere to build this fleet of meteorological satellites.



Figure 15. View from both apogees.

Figure 15 schematically illustrates the two possible apogees from which satellite images could be obtained for meteorological use, greatly aiding forecasting in the Southern Hemisphere. Therefore, an international collaborative project between South American and Oceanian countries would be highly suitable. Furthermore, Australia, Argentina, and Brazil possess excellent meteorological services and outstanding space technology infrastructure that could make these types of applications a reality.

In addition, the use of these satellites to cover communications in Antarctica could also be of interest to other countries that maintain bases on the frozen continent.

5. Conclusions

The use of Molniya orbits can be very useful for countries in the Southern Hemisphere. One of the best applications is meteorology and communications in Antarctica.

Between 2010 and 2015, the Pehuensat-2 satellite was developed based on the experience of Pehuensat-1, with the objective of gaining experience in a Molniya orbit over Antarctica, with apogee over the Drake Strait, where Argentina has satellite receiving stations (Tierra del Fuego Ground Station, located near the town of Tolhuin, of CONAE). This project could not be taken into orbit due to a lack of economic resources, but the development of the satellite reached the engineering model stage.

The massive development of cubesats by universities throughout the academic world makes it possible to revive the project today, with a preliminary mission to test the passive control capabilities in flight, image acquisition for meteorological applications, as well as its communications system, through a 3U cubesat that we call Pehuensat-4.

Use of AI tools declaration

The authors declare they have not used Artificial Intelligence (AI) tools in the creation of this article.

Acknowledgments

The authors wish to thank the Research Secretariat of the National University of Comahue for the grant provided to project PI-04-I285, which made this work possible.

Conflict of Interest

The authors declare no conflict of interest.

References

1. Chatters EP, Eberhardt B, Warner MS (2009) Chapter 6: Orbital Mechanics; the book AU-18 Space Primer, *Air University Press Maxwell Air Force Base*, Alabama; ISBN 978-1-58566-194.
2. Encyclopedia Wikipedia. Available from: https://en.wikipedia.org/wiki/Molniya_orbit.
3. Zadunaiski P (1998) Introducción a la Astrodinámica - Parte 1, *Comisión Nacional de Actividades Espaciales*, San Miguel, Argentina. Available from: https://www.argentina.gob.ar/ciencia/conae/publicaciones/introduccion-la-astrodinamica-teoria-y-metodos-numericos.
4. Millanao GE, Meliñir D, Canal C (2015), Transmisión de Imágenes Utilizando Protocolo Can; *VIII Congreso Argentino de Tecnología Espacial*. Buenos Aires, Argentina. Available from: https://aate.org/CATE_2015/CATE_2015_Trabajos.pdf.
5. Cuevas Mujica SA (2015) Control de Foco en una Cámara de Video, para Naves Aeroespaciales; *VIII Congreso Argentino de Tecnología Espacial*. Buenos Aires, Argentina. Available from: https://aate.org/CATE_2015/CATE_2015_Trabajos.pdf.
6. Simone D, Araoz M, Meroi C (2015) Protocolo de Comunicación para Enlace de Datos Satelital de Alta Velocidad; *VIII Congreso Argentino de Tecnología Espacial.* Buenos Aires, Argentina. Available from: https://aate.org/CATE_2015/CATE_2015_Trabajos.pdf.
7. Riquelme JL, Meroi Matinez C, Simone D, et al. (2014) Cálculo del enlace descendente en banda S y antena patch para el nanosatélite Pehuensat II, *2014 IEEE Biennial Congress of Argentina (ARGENCON)*, Bariloche, Argentina, 411–416. Available from: https://ieeexplore.ieee.org/document/6868528.
8. Quiroga JJ, Lassig J, Mendieta D (2013) Pehuensat-1: Development and Flight Test of a Nano Satellite. *Int J Space Technol Manage Innov* 3: 47–77. Available from: https://www.irma-international.org/article/pehuensat-1/99690/.
9. Uribe G (2011) Prediseño Estructural del Pehuensat-2; *VI Congreso Argentino de Tecnología Espacial*, San Luis, Argentina.
10. Lassig J, Garcilazo F, Robles A, et al. (2024) Desarrollo de un CubeSat como enseñanza extra curricular en Ingeniería, Parte 1: desarrollo mecánico. *Actas del Congreso Argentino de Enseñanza en Ingeniería*, San Juan, Argentina, Septiembre, 138–147. Available from: https://confedi.org.ar/cadi/cadi-caedi-2024/.
11. Hughes PC (1986) Spacecraft Attitude Dynamics. *John Wiley and Sons, Inc.*, *New York,* 297.
12. De León P (2003) Metodología de integración del proyecto PADE a bordo del transbordador espacial de la NASA; *Revista latinoamericana de ciencia y tecnología espacial; Volumen 2 N°1.* 1–9. Available from: https://www.aate.org/proyectos/pade/.
13. Lassig J, Quiroga J, Keil G (2007) Pehuensat-1: Final Configuration and Results of the First Month in Orbit; IAC-07-B4.1.08; *58th IAC Congress*, Hyderabad, India. Available from: https://www.proceedings.com/content/002/002817webtoc.pdf.



AIMS Press

© 2026 the Author(s), licensee AIMS Press. This is an open access article distributed under the terms of the Creative Commons Attribution License (https://creativecommons.org/licenses/by/4.0)